Proposal of design rules for improving the accuracy of selective laser melting (SLM) manufacturing using benchmarks parts

Sara Giganto

Department of Manufacturing Engineering, Universidad de León – Campus de Vegazana, León, Spain

Susana Martínez-Pellitero

Department of Manufacturing Engineering, Universidad de Leon – Campus de Vegazana, León, Spain

Eduardo Cuesta and Pablo Zapico

Department of Construction and Manufacturing Engineering, University of Oviedo, Oviedo, Spain

Joaquín Barreiro

Department of Manufacturing Engineering, Universidad de León – Campus de Vegazana, León, Spain

Abstract

Purpose – Among the different methodologies used for performance control in precision manufacturing, the measurement of metrological test artefacts becomes very important for the characterization, optimization and performance evaluation of Additive Manufacturing (AM) systems. In this study, several benchmark artefacts are designed and manufactured to evaluate the accuracy of the Selective Laser Melting (SLM) manufacturing process.

Design/methodology/approach – Artefacts consist of different primitive features (planes, cylinders, and hemispheres) on sloped planes (0º, 15º, 30º, 45º) and stair-shaped and sloped planes (from 0º to 90º, at 5º intervals), manufactured in 17-4PH stainless steel. The artefacts were measured optically by a structured light scanner to verify the Geometric Dimensioning and Tolerancing (GD&T) of SLM manufacturing.

Findings – The results provide design recommendations for precision SLM manufacturing of 17-4PH parts. Regarding geometrical accuracy, it is recommended to avoid surfaces with 45º negative slopes or higher. On the other hand, the material shrinkage effect can be compensated by resizing features according to X and Y direction.

Originality – No previous work has been found that evaluates accuracy when printing inwards (pockets) and outwards (pads) geometries at different manufacturing angles using SLM. The proposed artefacts can be used to determine the manufacturing accuracy of different AM systems by resizing to fit the build envelope of the system to evaluate. Analysis of manufactured benchmark artefacts allows to determine rules for the most suitable design of the desired parts.

Keywords

17-4PH stainless steel; Benchmark artefacts; Design rules; Manufacturing accuracy; Metal additive manufacturing; Optical inspection; Selective Laser Melting (SLM)

1. Introduction

In recent years, the capabilities of metal-based Additive Manufacturing (AM) methods have been improved significantly, and these technologies have emerged as viable processes for direct manufacturing of metal parts. Among the different AM techniques,

the Selective Laser Melting (SLM) is based on layer-by-layer creation of the final parts by melting metal powder particles with a laser energy source. The ability to manufacture free-form and complex geometries in metallic materials, as well as the possibility to topologically optimize and lighten components, make the SLM process of great interest in areas such as medical, automotive and aerospace. In these areas, parts and components must meet high performance specifications, including mechanical/thermal/chemical properties, as well as good dimensional and surface finish requirements.

Regarding dimensional quality, the main impact of metal AM processes on manufactured geometry is the distortion of the produced parts (Leach et al., 2019). The high temperature gradient and rapid cooling produced during the SLM process cause residual stresses in the manufactured parts, which vary based on several factors such as process parameters, material properties, geometry of printed parts, and support structures (Yadroitsev et al., 2015). There is a real need to optimize the quality of additively laser manufactured metal parts by developing design methodologies and guidelines for geometrical design (Chahal et al., 2020). Geometrical and dimensional measurement implies an important limitation to accelerate the AM industrial adoption due to difficulties in adapting current measurement techniques and systems. Test artefacts play an important role in the diagnosis and characterization of metal AM processes and machines (Moylan et al., 2012) (Moylan et al., 2014). In their study, Carmignato et al. (2020) provided guidelines for the selection, use and development of dimensional artefacts.

According to Mahesh (2004), benchmark artefacts for evaluating AM processes can be classified into three groups according to their main purpose: “Geometrical benchmarks” used to check geometrical (Rebaioli and Fassi, 2017) and/or dimensional performance (ISO/ASTM 52902, 2019), accuracy (dimensional (Pessard et al., 2008) and/or geometric (Cooke and Soons, 2010)), tolerances (Hanumaiah and Ravi, 2007)

(Rupal et al., 2020), repeatability (Delgado et al., 2009), and surface finish (Strano et al., 2013)); "Mechanical benchmarks" used to characterize mechanical properties (shrinkage (Ning et al., 2006), deformation, tensile and compressive strengths, and creep characteristics); and "Process benchmarks" used to define the optimal process parameters (Calignano et al., 2017) (laser power, scanning speed, layer thickness, part orientation (Grimm et al., 2015), support structures, etc.). There are also artefacts that combine several purposes, such as the one designed by Taylor et al. (2021) to evaluate dimensional accuracy, distortion, residual stress, geometry-specific microstructure, chemistry, surface integrity, powder removal and mechanical properties. Some artefacts have also been designed to assess the detailed capability and geometrical limitations of metal AM systems (Teeter et al., 2015), as well as to evaluate the entire manufacturing process. An example is the study conducted by Vandenbroucke and Kruth (2007) in which they designed three artefacts for evaluating the SLM process by testing the influence of the slope angle, difference between top and bottom surfaces, feasibility for achieving small details, and process accuracy. Further examples are the artefact proposed by Campanelli et al. (2010) to assess the capacity of the SLM process in terms of dimensional accuracy and minimum feasible feature size, the artefact designed by Subbaian Kaliamoorthy et al. (2020) to test the ability to SLM manufacture cooling channels to support mould manufacturing, and the three test artefacts designed by Townsend et al. (2018) to provide comprehensive information relating to AM surfaces.

Other research has focused on the study of artefacts to compare different metal AM processes. Kruth et al. (2005) tested the accuracy, material, mechanical properties, speed, and reliability of the Selective Laser Sintering (SLS) and SLM processes. Castillo (2005) measured the accuracy, capability, geometrical limitations, and the ability to build outgoing planes at different angles of four metal AM technologies. Ghany and Moustafa

(2006) used a "real world" part to compare the visuals, microstructure, chemical composition, mechanical properties, and processing costs of five different metal AM technologies. Minetola et al. (2020) designed an artefact to evaluate and compare the dimensional accuracy of two Powder Bed Fusion (PBF) systems for metallic materials using ISO International Tolerance grades. On the other hand, Yasa et al. (2014) designed a benchmark to compare four different suppliers of Laser Beam Melting (LBM) machines through the analysis of surface quality, dimensional accuracy, geometrical resolution, density, hardness, the need of support structures, and process limits. Moshiri et al. (2019) presented the methodology and results of an extensive benchmarking of five different LBM machines to understand the influence of each machine on the final quality of the designed artefact.

According to Scaravetti et al. (2008), test artefacts must not only evaluate process limitations, but must also include features to allow an iterative process optimization. In addition, the qualification procedure should allow the identification and quantification of defects, as well as the determination of their source. To achieve this, the test artefacts should have simple geometrical shapes (allowing easy control and perfect definition of the geometry), not require post-processing or manual intervention (e.g. there should be no supporting structures), and allow measurement repeatability (Moylan et al., 2012). In this regard, Rupal et al. (2018) provided a systematic methodology for geometrical benchmark test artefact design to evaluate the geometrical behaviour of AM processes.

None of the studies previously mentioned have analysed the accuracy of additively manufacturing metal benchmark parts with different canonical features (inwards and outwards) built on planes at different inclinations with respect to the printing axes of AM technology. Locating these canonical features on inclined planes constitutes a major additional complexity in conventional milling machines (it requires special

clamping, tool/head rotation, etc.), but this is not a problem for AM technologies, unless the inclination is excessive. Therefore, the advantage of studying geometries in sloped planes is of great interest for AM. However, previous research of other authors in this field use benchmark parts with geometrical features only in vertical/horizontal planes, without considering inclined planes. Moreover, not all types of geometrical primitives are considered in previous research. Therefore, our study focuses on dimensional and geometrical evaluation of different geometries on sloped planes manufactured by SLM, as well as analysing the manufacturing accuracy of stair-shaped and sloped planes. Likewise, this study will allow to generate design rules for the SLM metal parts manufacturing.

Regarding measurement techniques, the use of a Coordinate Measuring Machine (CMM) to measure dimensions and shape is complicated by the specific characteristics of the metal AM parts, due to surface texture and complex shapes. The typical high roughness of these surfaces produces significant deviations among measurements made with different contact or optical dimensional measurement systems (Leach et al., 2019). Rivas Santos et al. (2020) concluded that CMMs may not be the most effective system for carrying out reference measurements of AM parts, with optical systems (such as a structured light scanner among others) being more appropriate. In this work, a structured light scanner is used to obtain GD&T measurements on the artefacts. This 3D scanner achieves a very high precision, especially important on parts with the typical SLM surface finish (Giganto et al., 2020).

The context of this study is the evaluation of small-size SLM parts that could be manufactured without additional drawbacks except the inclination, and that could be inspected by optical systems without the common occlusion problem. The main object of this research is to study the influence of the inclination and the type of geometry.

2. Materials and methods

Figure 1 shows the methodology for analysing the geometrical and dimensional accuracy of parts manufactured by SLM technique. In the first step, the benchmark artefacts were designed considering the restrictions of the SLM process and machine, and the optical measurement requirements. Once the parts were manufactured in 17-4PH, they were Heat Treatment (HT) post-processed to relieve residual stresses caused during the manufacturing process. After splitting the artefacts from the build-plates, they were digitized using a structured light scanner. Finally, the GD&T measurements and 3D comparisons between the nominal CAD and the scanned point clouds were performed.

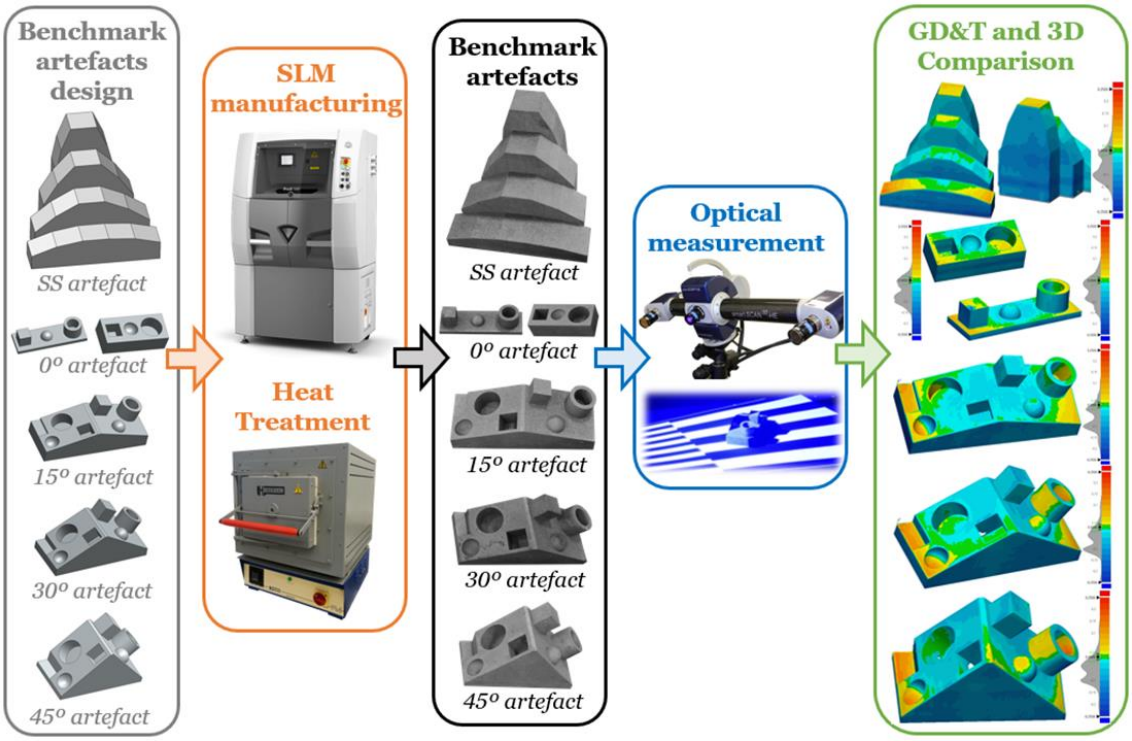

Figure 1 Methodology for optical evaluation of ad-hoc artefacts additively manufactured using SLM.

2.1. Benchmark artefact designs

The artefacts were designed according manufacturer recommendations regarding to manufacturing conditions, as well as the design recommendations of the authors cited in the introduction section:

- Primitive features to allow a perfect definition and easy verification.
- Suitable size features to check SLM machine performance considering the machine capacity and the maximum area per layer (no more than 50% of the build-plate surface to prevent its deformation, according to the manufacturer's recommendations).
- Containing both inwards (pockets) and outwards (pads) geometries.
- No hanging surfaces to avoid the requirement of support structures (therefore preventing removal and polishing of supports).
- Easy to measure by optical systems considering, among other aspects, occlusion problems, minimum size, and maximum depth of inwards features.

Figure 2 shows the first benchmark artefact designed in this study for GD&T evaluation. The Sloped and Stair-shaped surfaces (SS) artefact consists of 18 sloped planes (12x12 mm) from 5º to 90º, increasing at 5º intervals (Pl_5 to Pl_{90}), 4 planes at 0º (Pl_0^1 to Pl_0^4), and 5 planes at 90º (Pl_{90}^1 to Pl_{90}^5).

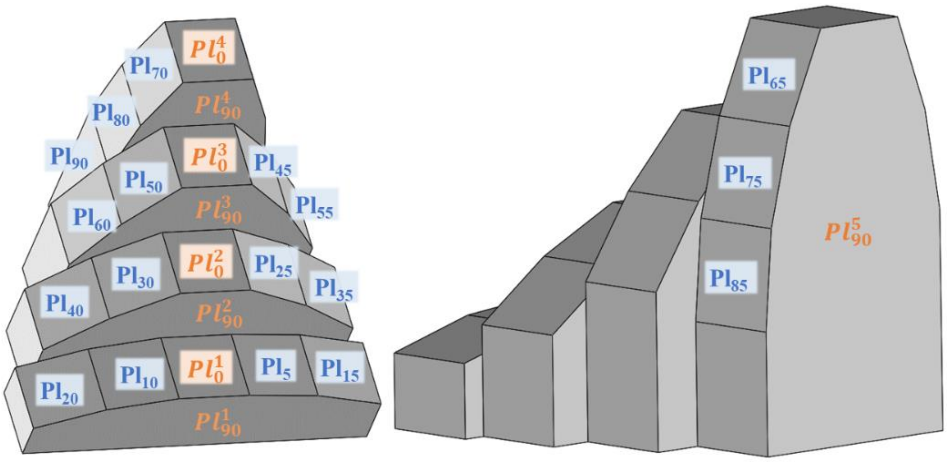

Figure 2 Planes designation of the Sloped and Stair-shaped surfaces (SS) artefact.

The other benchmark artefact consists of three inwards and three outwards canonical features (cube, hemisphere, and cylinder) built on inclined planes at 0º (Figure 3(a)), 15º (Figure 3(b)), 30º (Figure 3(c)) and 45º (Figure 3(d)). The cube dimensions are 10 mm side, the hemisphere is 10 mm diameter, the inwards cylinder is 15 mm diameter and 10 mm depth, and the hollow cylinder is 15 mm outer diameter, 10 mm inner diameter and 10 mm height. The use of planes with different inclination leads to modify the thickness of the artefacts base. However, the main objective of this research is to study the influence of the inclination of the canonical features in the manufacturing process layer by layer. Likewise, in future research it would be interesting to develop benchmark parts with uniform thickness or use topological optimization to improve the results.

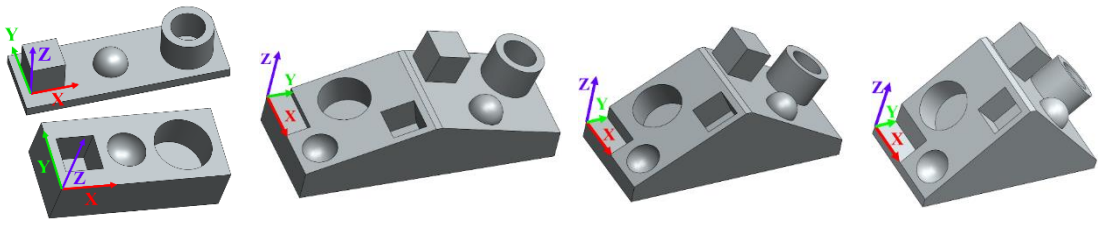

(a) (b) (c) (d)

Figure 3 CAD of benchmark artefact designs to evaluate GD&T of SLM parts: outwards and inwards features on a plane at: (a) 0º, (b) 15º, (c) 30º and (d) 45º.

Figure 4 shows the features designation of the 15º artefact as an example. The 0º, 30º and 45º artefacts have a similar designation. Planes of the inwards and outwards cubes are designated according to the coordinate axis normal to them, and the distance to the coordinate's origin (1 if the closest and 2 if the furthest to the origin).

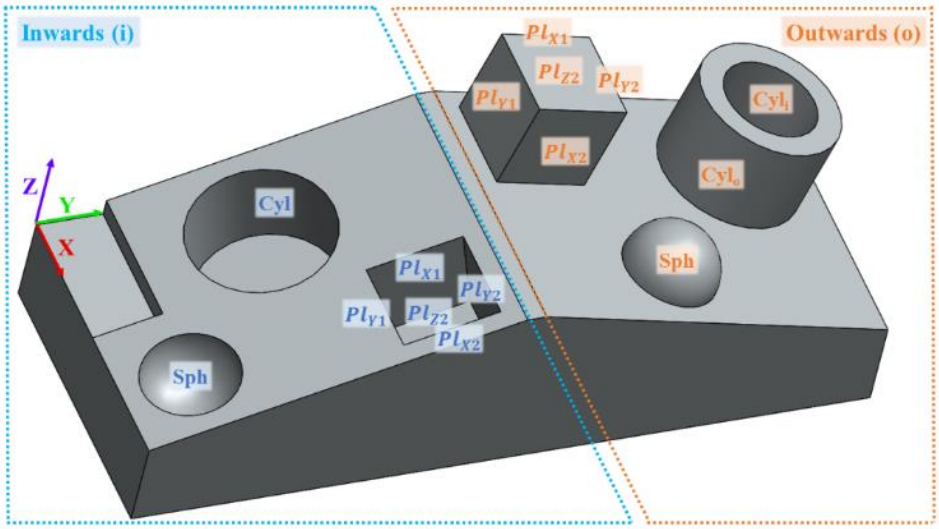

Figure 4 Features designation of the 15º artefact.

2.2. SLM manufacturing process and HT post-process

A ProX® 100 (3DSystems) machine was used to manufacture the benchmark artefacts. This metal SLM machine works with a fibre laser of 1070 nm wavelength. The maximum power of the laser is 50 W, but this parameter was optimized to 38 W based on a previous work (Zapico et al., 2018). In order to achieve good mechanical properties (Kudzal et al., 2017) and high-density parts (Rashid et al., 2018), the used scanning strategy was the hexagonal, as recommended by the SLM machine manufacturer and other researchers. This strategy involves the manufacture of each layer using hexagonal patches of 5000 µm side and an overlap between them of 50 µm (standard values). The layer thickness and scanning speed parameters were set at 30 µm and 140 mm/s, respectively. During the process, the manufacturing chamber was inertized with nitrogen supplied at 7 bars of pressure by a generator connected to it. The build envelope of the SLM machine is

100x100x100 mm. The repeatability and typical accuracy are 20 µm (in the three axes X, Y, Z) and ±0.1-0.2% (±50 µm minimum), respectively.

The metal powder was 17-4PH stainless steel supplied by 3DSystems. The chemical composition is (weight %): 15-17.5 Cr, 3-5 Ni, 3-5 Cu, <1 Si, <1 Mn, 0.15-0.45 Nb, and balance Fe. It is a precipitation-hardened (PH) martensitic stainless steel that offers high strength and hardness with excellent corrosion resistance. It is commonly used in applications that require good thermal properties and excellent mechanical properties at high temperatures (up to 300ºC). This alloy is used to produce industrial grade prototypes or spare parts in sectors such as surgical instruments, aerospace, general metallurgy, the chemical industry, energy, the petrochemical industry, and high-wear components.

The six artefacts were SLM manufactured on three build-plates (occupying 35% of the total plate surface) (Figure 5) to reduce the consumption of material and save time.

Figure 5 Artefacts after the SLM manufacturing process.

After SLM manufacturing of the artefacts, the 17-4PH parts/build-plate sets were subjected to stress relieving HT according to recommendations of the manufacturer and others researches (Sun et al., 2018). This treatment prevents distortion of the parts and is the most effective method to relieve these residual stresses (Li et al., 2018). This post-processing is beneficial for homogenizing the microstructure, improving the mechanical properties, and increasing ductility by reducing the tensile strength of the SLM parts

(Pidge and Kumar, 2020). Therefore, the stress relieving HT acquires a great relevance after manufacturing SLM parts and before separating them from the build-plate.

In addition to HT post-processing, some researchers such as Maamoun et al. (2018) or Malý et al. (2019) achieved a decrease in residual stresses due to preheating of the build-plate before starting the SLM manufacturing process. Other researchers have rescanned (double scanning of each layer) (Xiao et al., 2020) or optimized process parameters (Jiang et al., 2020) as a method to reduce these residual stresses.

In our study, the manufactured parts were HT post-processed holding the artefact at 650ºC for 2 hours, and air cooling (usual for 17-4PH material). Finally, the parts were split from the build-plate by wire electrical discharge machining.

2.3. Optical measurement

A structured blue-light scanner based on the fringe pattern projection technique was used to evaluate the artefacts. The Breuckmann smartSCAN^{3D}-HE (currently AICON SmartScan) consists of a projection unit and a two cameras acquisition unit, located on each side of the projector (right and left). Thanks to the miniaturized projection technique, this 3D scanner is characterized by a fast data acquisition and a high level of precision. The depth information is obtained by triangulation. The projection system applies an appropriate sequence of blue-light fringe patterns (with a 28 Mpx resolution and 550 ANSI lumen) onto the part, depending on the characteristics of the object to be measured. The two-camera system (with a resolution of 4 Mpx/camera) captures the projected fringe pattern at a predefined viewing angle according to the configured Field of View (FOV). The diagonal length of the measurement volume determines the FOV size. For this study, a 125 mm FOV was used since it is the smallest FOV that allows for the entire volume of the designed artefacts to be captured. The measuring volume for this FOV is 95x95x60

mm with an X and Y resolution of 50 µm, a resolution limit Z of 5 µm, and a feature accuracy of 9 µm.

The scanner was previously calibrated with the procedure recommended by the manufacturer. Calibration and part scanning operations were carried out with the Optocat® software. About 15 scans/part were required for full scanning of the benchmark artefacts. All artefacts were scanned on the same day under the same conditions.

2.4. Geometric dimensioning and tolerancing and 3D comparison

Point clouds resulting from the optical digitizing were imported in Geomagic® Control X™ inspection software. In the first step, the point clouds were aligned with the nominal CAD using the best-fit option. The best-fit alignment tool allowed to align measured data to reference data using the overlapping regions between them. For this, all the measured data were used except the noisy poly-vertices and a maximum number of 30 registration iterations. Then, the different geometries were reconstructed as features (plane, sphere, and cylinder) also using the best-fit adjustment method (least squares algorithm), and the 3*Sigma filtering method to remove outlier data larger than 3 times the standard deviation. In the next step, a 3D comparison was made between the nominal CAD and the point cloud for each artefact. Finally, GD&T values were evaluated using virtual features.

3. Results and discussion

This section presents a 3D comparison between the digitized artefacts and their nominal CAD, as well as the most relevant results derived from the geometrical and dimensional analysis.

3.1. 3D comparison between digitized geometry and nominal CAD

Figure 6 shows graphically the 3D comparison between the nominal CAD and the scanned point clouds. The SS artefact comparison (Figure 6(a)) shows a decrement according to the X and Y directions (blue surface). The green colour indicates the best fit surfaces between the SLM part and the nominal CAD design (Figure 6). A common trend is observed: a negative deviation in the part centre becomes positive towards the part ends, according to the Y axis (Figure 6(b), 6(c), 6(d) and 6(e)). This error is due to residual stresses caused during the SLM process that tend to deform parts as a concave-shaped curve when separated from the build-plate (Li et al., 2017). Likewise, according to studies carried out by Mercelis and Kruth (2006), the parts removed from their build-plates exhibit a basic residual stress distribution in the Z direction consisting of a tensile stresses zone just below the top surface, followed by a large compressive stress zone, ending again with a tensile stresses zone at the bottom.

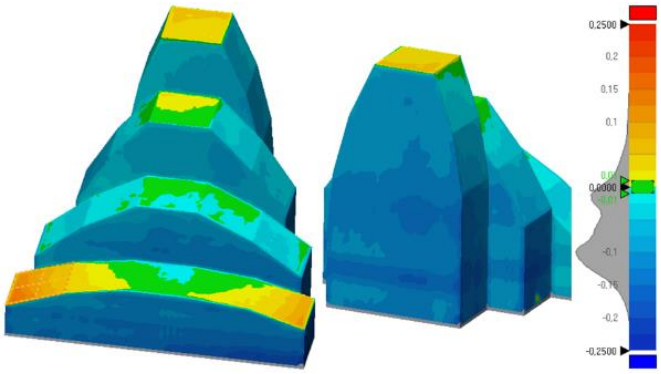

(a)

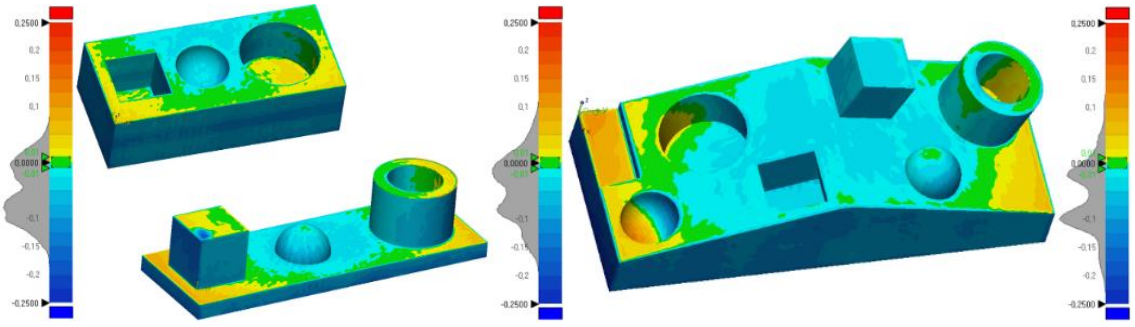

(b) (c)

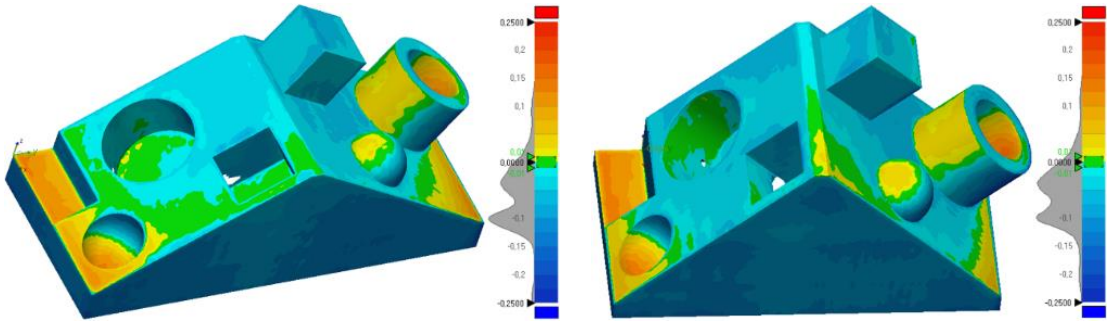

(d) (e)

Figure 6 3D comparison between the designed nominal CAD and the artefacts scanned point clouds: (a) SS, (b) 0º, (c) 15º, (d) 30º and (e) 45º.

The base planes of the five artefacts suffer similar deviations, ranging from positive values at the ends to negative values at the centre. Regarding the cylinder and hemisphere features on the sloped faces, the deviations are higher (yellow surface) when the base plane angle increases (Figure 6(b), 6(c), 6(d) and 6(e)). The trend is similar for the cube faces (negative deviations), except for the cube in the negative sloped face in which the deviation is positive. Also, when increasing the base plane angle, the standard deviation value of the 3D comparison is also higher (Table I).

Table I Standard deviation and RMS of the 3D comparison between the designed CAD and the artefacts points clouds.

Artefact	**SS**	**0^{o}_{o}**	**0^{o}_{i}**	**15º**	**30º**	**45º**
Standard Deviation (mm)	0.0610	0.0575	0.0518	0.0625	0.0674	0.0644
RMS (mm)	0.0883	0.0726	0.0736	0.0866	0.0890	0.0890

The Root Mean Square deviation (RMS) value, which is a combination of the average value of the form error and its dispersion, shows an increasing trend when increasing the base plane angle (Table I). Furthermore, Figure 6 shows that the average value reaches negative deviations in all the artefacts, due to the aforementioned shrinkage effect.

3.2. Analysis of geometrical errors

The standard deviation of the geometrical features in the benchmark artefacts was used to analyse the form specifications, instead of using the form error parameter (flatness, cylindricity and sphericity, according to ISO 1101:2017). Standard deviation is a representative form specification parameter for optical measurements since it reduces the influence of spurious points. These points are intrinsic to optical methods due to brightness, reflections, etc.

3.2.1. Sloped and Stair-shaped surfaces (SS)

The standard deviation of planes at different manufacturing angles (SS artefact) shows a decreasing trend when increasing the angle (Figure 7). These results are due to the stair effect (Das et al., 2015) caused by the layer by layer additive process. This effect depends on both the layer thickness and the build direction (Leach et al., 2019). The highest deviation value is 0.0149 mm which corresponds to Pl_5; the lowest values are 0.0088 and 0.0095 mm which correspond to Pl_{85} and Pl_{90}, respectively.

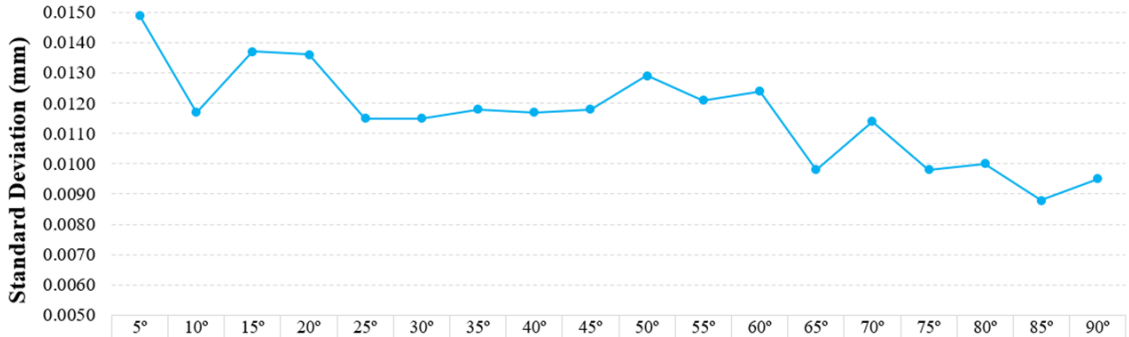

	5°	10°	15°	20°	25°	30°	35°	40°	45°	50°	55°	60°	65°	70°	75°	80°	85°	90°
Sloped planes	0.0149	0.0117	0.0137	0.0136	0.0115	0.0115	0.0118	0.0117	0.0118	0.0129	0.0121	0.0124	0.0098	0.0114	0.0098	0.0100	0.0088	0.0095

Figure 7 Standard deviation of SS artefact sloped planes.

Figure 8 shows the standard deviation of both the 0º (Figure 8(a)) and 90º (Figure 8(b)) planes of the stair-shaped planes in the SS artefact. The standard deviation value of the 0º and 90º planes ranges from 0.009 to 0.015 mm.

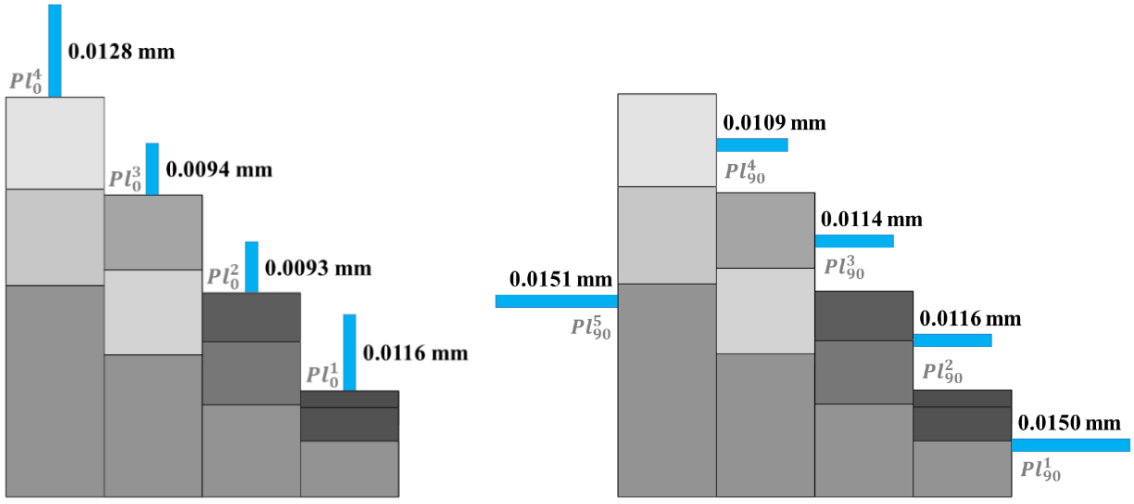

(a) (b)

Figure 8 Standard deviation of SS artefact stair-shaped planes: (a) 0º and (b) 90º.

3.2.2. Outwards and inwards features

Figure 9 shows the standard deviation of the outwards features. Regarding the planes (Figure 9(a)), the results are similar for both benchmark artefacts and different surfaces, except in the case of the Pl_{Y2}^{o}. The Pl_{Y2}^{o} (corresponding to the cube negative sloped plane) presents a great variation in the 45º artefact, with a standard deviation value of 0.0261 mm compared to values close to 0.0110 mm of the other artefacts. This is because 45º is the limiting angle from which the SLM machine manufacturers recommend adding supporting structures for negative sloped planes. Regarding the spheres and hollow cylinders (Figure 9(b)), there are no significant differences for the smallest angles (0º and 15º), however there is an increasing trend from 30º.

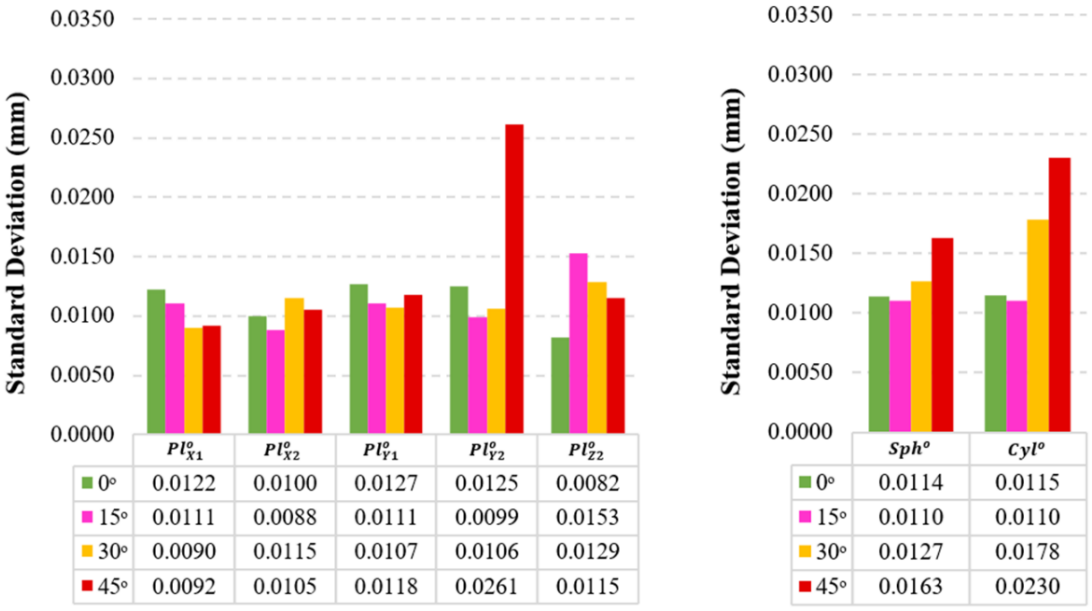

(a) (b)

Figure 9 Standard deviation of outwards features: (a) planes, (b) sphere and cylinder.

As seen in the 3D comparison (Figure 6), the inwards features have been captured with enough points to define them with accuracy. The form specifications of the inwards features present a similar trend among the different artefacts, with some high deviations (Figure 10). The highest standard deviation value corresponds to the Pl^i_{Y2} in the 45º artefact (0.0338 mm) followed by the same face in the 30º artefact (0.0260 mm) (Figure 10(a)). These results correspond to the negative sloped planes error already mentioned in the previous section. Regarding the inwards spheres and cylinders (Figure 10(b)), the values are similar (less than 0.015 mm) except for the cylinders in the 45º artefact, which reach deviations close to 0.020 mm.

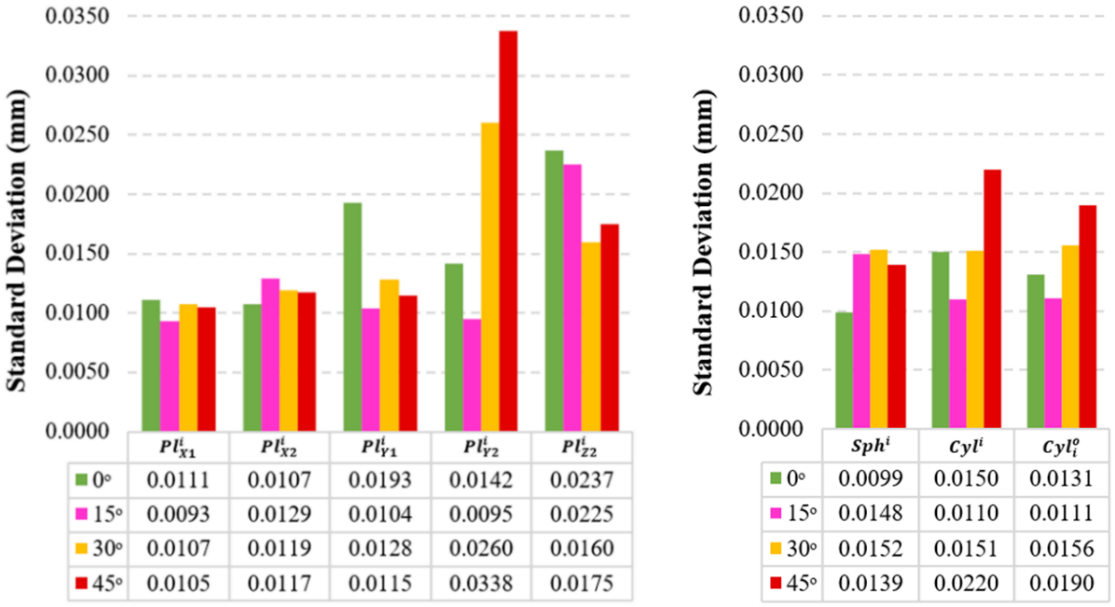

(a) (b)

Figure 10 Standard deviation of inwards features: (a) planes, (b) sphere and cylinders.

At 45º slope, the geometrical error is higher. However, some differences are encountered among the several geometrical features. The reason is that the portion of surface unsupported at 45º is different in each case (cube, cylinder, sphere) as shown highlighted in red in Figure 11. The worst case is the cube both inwards (Pl^i_{Y2}) and outwards (Pl^o_{Y2}), since the face at 45º is completely free (Figure 11). In the case of the cylinder, only a small portion of the surface is completely free and the rest of surface is somehow resting in previous layers.

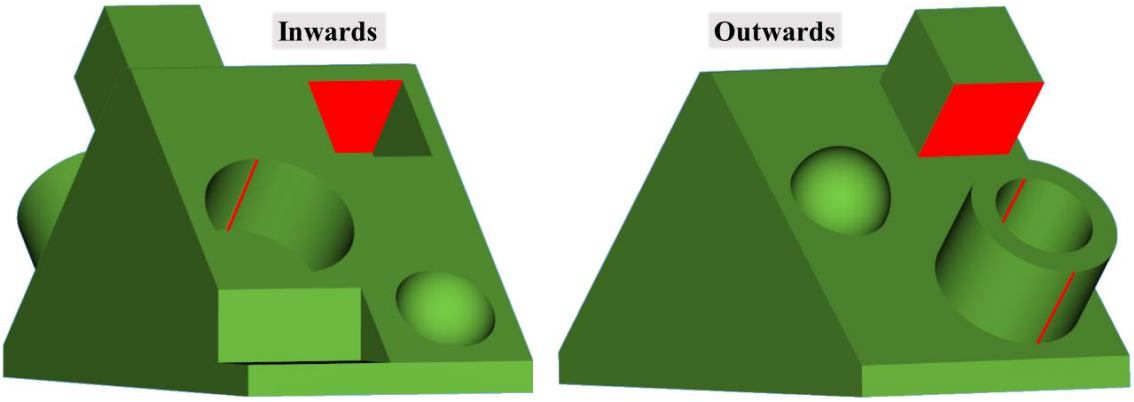

Figure 11 Surfaces with 45º negative slopes of the inwards and outwards features of the 45º artefact.

3.3. Analysis of dimensional errors

The results obtained in this section were calculated with regard to the reference values (CAD nominal design) to evaluate the SLM manufacturing accuracy.

3.3.1. Sloped and Stair-shaped surfaces (SS)

No clear or remarkable trend is observed in the analysis of the angle deviation respect to the nominal value for the sloped planes. As Figure 12 shows, the angle deviation values are negligible except for 15º and 20º planes, whose error reaches 0.49º and 0.61º deviation values, respectively.

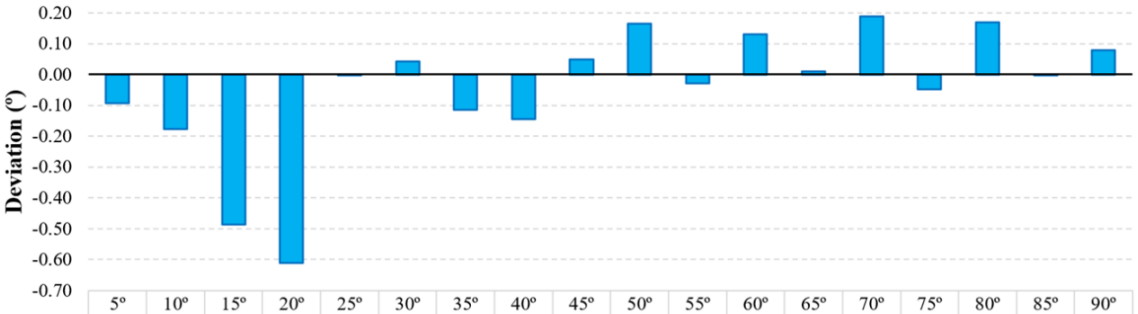

	5º	10º	15º	20º	25º	30º	35º	40º	45º	50º	55º	60º	65º	70º	75º	80º	85º	90º
Angle	-0.093	-0.177	-0.486	-0.610	-0.002	0.042	-0.115	-0.144	0.049	0.164	-0.029	0.129	0.010	0.189	-0.049	0.169	-0.003	0.078

Figure 12 Manufacturing angle deviation of the SS artefact sloped planes.

Figure 13 shows the dimensional deviations of the SS artefact stair-shaped surfaces. To measure the steps height, the linear distances (normal direction from the centre point of first geometry) from Pl_0^1 to Pl_0^2 (Z1), Pl_0^3 (Z2) and Pl_0^4 (Z3) were taken. Likewise, to obtain the steps width, the distances from Pl_{90}^1 to Pl_{90}^2 (Y1), Pl_{90}^3 (Y2), Pl_{90}^4 (Y3) and Pl_{90}^5 (Y4) were measured (Figure 13(a)). In order to properly compare the results, the dimensional deviation values (Figure 13(b)) were calculated based on the measured distance. The steps height deviations show an increasing trend with the part height (about 0.010 mm on each step as shown in Figure 13(b)). However, considering that this regular increase with the part height is a deviation value lower than the scanner resolution, it

should be neglected. In the case of the Y direction, in addition to being very small deviation values, they do not show any trend.

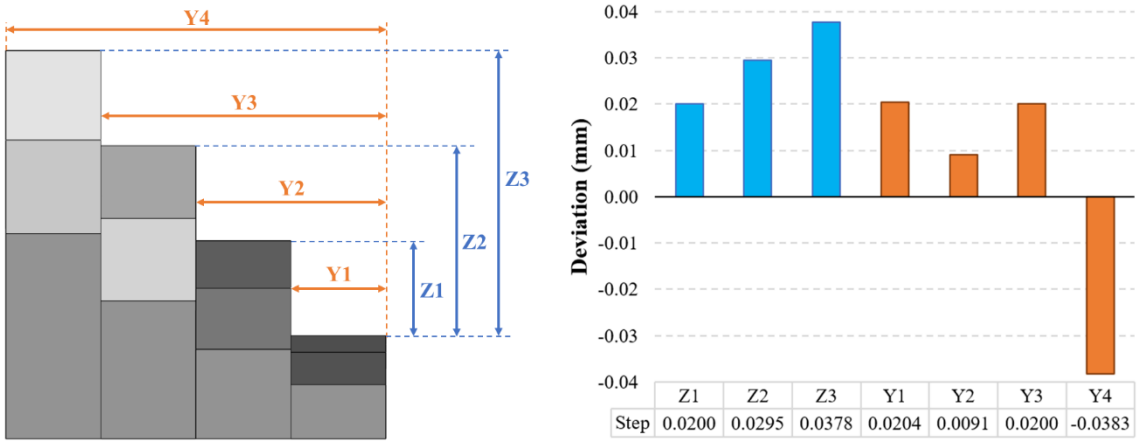

(a) (b)

Figure 13 (a) SS artefact dimensions on the designed CAD and (b) deviations in the step's height and width.

3.3.2. Outwards and inwards features

Figure 14 shows the cube's dimensions (X, Y, Z) for both inwards and outwards features. Regarding the distances between parallel faces of the outwards cubes, similar contractions are observed whatever the manufacturing angle and the X or Y direction. These deviations are around 0.15 mm, a significant value to be compensated in the design phase of the SLM parts. However, the deviations along the Z axis of the outwards cubes (or cubes height) are positive and do not reach 0.015 mm in any of the analysed angles. A similar trend occurs for inwards features, but with opposite sign (Figure 14). Dimensional deviations of inwards cubes according to Z direction are less than 0.025 mm. On the other hand, X and Y dimensional deviation of the inwards cubes are similar and less than 0.10 mm, except for the Y dimension of the cubes manufactured at 30º and 45º, whose dimensional deviations reach 0.15 and 0.20 mm, respectively.

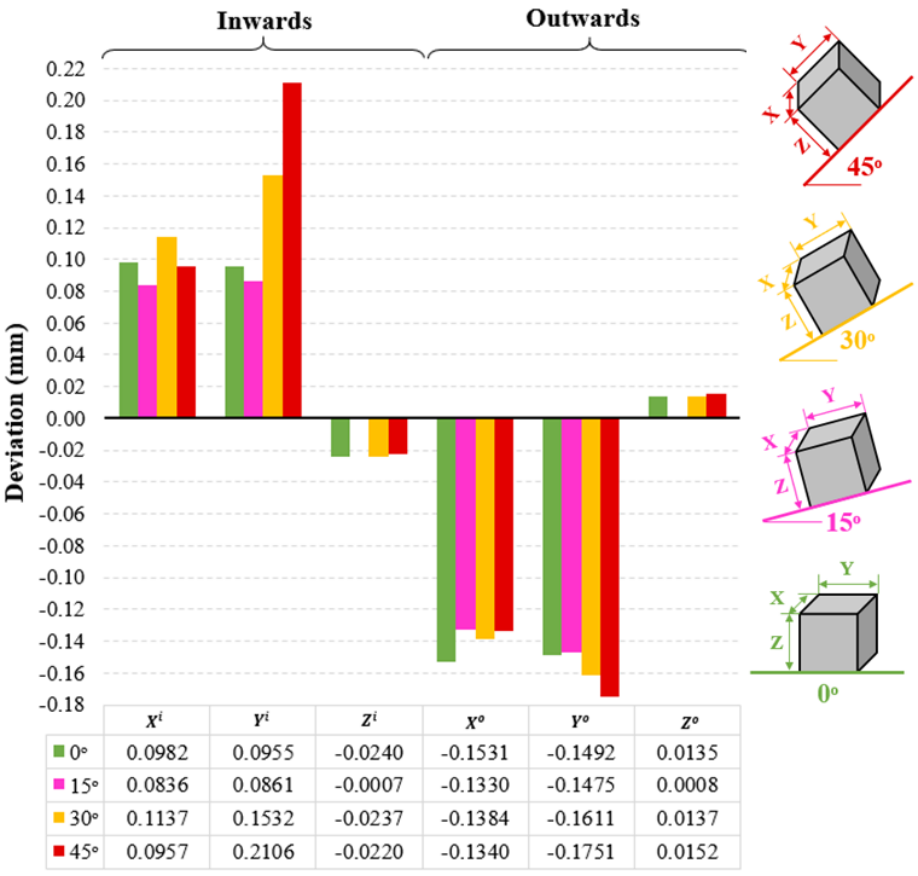

	x^i	y^i	z^i	x^o	y^o	z^o
0º	0.0982	0.0955	-0.0240	-0.1531	-0.1492	0.0135
15º	0.0836	0.0861	-0.0007	-0.1330	-0.1475	0.0008
30º	0.1137	0.1532	-0.0237	-0.1384	-0.1611	0.0137
45º	0.0957	0.2106	-0.0220	-0.1340	-0.1751	0.0152

Figure 14 Dimensional deviations of the artefacts' cubes.

Figure 15 shows the hemisphere and cylinder diameters for both inwards and outwards features. For the outwards cylinders, a significant contraction around 0.17 mm is observed for cylinders manufactured at 0º and 15º, increasing to 0.22 mm for cylinders manufactured at the largest angles (30º and 45º). Similarly, the outwards spheres diameters show a contraction around 0.18 mm, independently the manufacturing angle. Regarding the inwards features, deviations in the cylinders and spheres diameters show a decreasing trend when increasing the manufacturing angle.

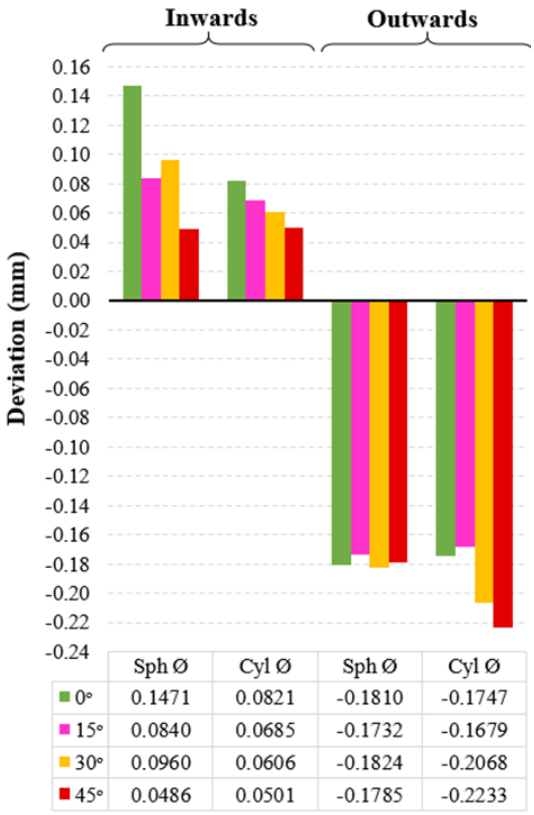

	Sph Ø	Cyl Ø	Sph Ø	Cyl Ø
0°	0.1471	0.0821	-0.1810	-0.1747
15°	0.0840	0.0685	-0.1732	-0.1679
30°	0.0960	0.0606	-0.1824	-0.2068
45°	0.0486	0.0501	-0.1785	-0.2233

Figure 15 Dimensional deviations of the artefact's spheres and cylinders.

Regardless of the base plane angle (0º, 15º, 30º, 45º), the features present high dimensional deviations along the X and Y axes (parallel directions to the base plane) and low deviations in height (Z axis or perpendicular direction to the base plane). The X and Y dimensions of the outwards features are smaller than the nominal CAD values due to the shrinkage effect caused by the SLM cooling process. The steep temperature gradient due to localized heating and cooling by the heat source moving causes a thermal expansion and contraction of the material and, consequently, the parts deformation (DebRoy et al., 2018). At design stage, it is recommended to resize 17-4PH parts manufactured using the SLM technique considering these dimensional deviations.

4. Conclusions

Several researchers have designed test parts to evaluate the performance of metal AM systems, using benchmark parts with some geometrical features in vertical/horizontal

planes. However, so far manufacturing geometrical features (outwards and inwards) on planes at different inclination has not been considered. Manufacturing features on inclined planes constitutes a major additional complexity in conventional machine tools, but this is not a problem for AM technologies (unless the inclination is excessive). Therefore, the advantage of studying geometries in sloped planes is of great interest for AM, and that is precisely what this work focuses on. This study evaluates the geometrical and dimensional quality of the SLM parts and proposes a practical guide to design this type of parts.

According to the obtained results, it is recommended to consider the following conclusions when designing 17-4PH stainless steel parts to be manufactured using the SLM technology:

- Regardless of the slope angle (from 0º to 90º), the manufactured planes achieve good geometrical accuracy, generally not exceeding 15 µm of standard deviation. In addition, an increasing trend is observed in the geometrical error when reducing the manufacturing angle. This is directly related to the typical stair effect of layer-addition-based manufacturing techniques.
- Considering the angle deviation of the sloped planes (from 0º to 90º), it is recommended to avoid 15º and 20º sloped surfaces to maintain the dimensional accuracy.
- The manufacture of stair-shaped surfaces provides good geometrical and dimensional accuracy.
- The geometrical error of the spherical and cylindrical features, both inwards and outwards, shows an increasing trend when increasing the base plane angle. Regarding the cubes faces, both inwards and outwards, the high geometrical error of 45º negative sloped surface stands out. Therefore, from the point of view of

geometrical accuracy, it is recommended to avoid surfaces with 45º negative slopes or higher.

- The dimensional analysis of the features manufactured in sloped planes shows an important error in the X and Y direction, being negligible in the Z direction. These dimensional errors are due to the parts shrinkage caused by the rapid cooling process, resulting in larger inwards features and smaller outwards features. The shrinkage percentage of the material depends on the part size, as the part size decreases the shrinkage percentage increases. For features sizes similar to those in this study, when manufacturing parts for applications with narrow dimensional tolerances, it is recommended to resize the features according to the values in Table II.

Table II Resizing of features as a function of the slope angle of the base plane.

Feature resizing (%)						
	↑Outwards			**↓Inwards**		
Artefact angle	**Cubes XY size**	**Spheres Ø**	**Cylinders Ø**	**Cubes XY size**	**Spheres Ø**	**Cylinders Ø**
0º	1.50	1.80	1.20	-1.00	-1.50	-0.70
15º	1.50	1.80	1.20	-1.00	-1.00	-0.60
30º	1.50	1.80	1.50	-1.50	-1.00	-0.50
45º	1.50	1.80	1.50	-1.50	-0.50	-0.40

- Regarding the geometrical accuracy of features manufactured on sloped planes, the most influential factor is the building angle. Better results are achieved for small angles. In the case of dimensional accuracy, in addition to the manufacturing angle, the type of geometry is another important factor.

The benchmark artefacts proposed in this work must be resized to fit the build envelope of the system to be evaluated.

As future works, it is proposed to assess the influence of the dimensions (height, width, length, diameter, thickness, etc.) of different geometrical entities (cube, sphere, cylinder, cone, etc.) through methodical experimentation using a factorial approach of Design Of Experiments (DOE), which allows statistical significance and the development of a mathematical model. In this way, the study would be extended by providing the sensitivity of these parameters in SLM manufacturing. As well as analysing the SLM printing of thinner walls and overhangs, features that are more sensitive to distortion induced by residual stress generated during the manufacturing process.

It is also proposed to analyse the SLM manufacturing accuracy using different laser scanning strategies (such as normal or concentric), as well as different post-processes (such as laser rescanning, optimization of other process parameters or the preheating of the build-plate) to reduce residual stresses produced during the AM. These process and post-process variables could affect to geometrical and dimensional deformations of the manufactured parts.

Likewise, it is proposed as future work to design and manufacture test parts to determine the minimum feature size manufactured by SLM, in order to define the limits of this technology. In addition to the geometrical size, the influence of the build direction and the type of feature (inward or outward) on the manufacturing precision must also be analysed.

References

Calignano, F., Lorusso, M., Pakkanen, J., Trevisan, F., Ambrosio, E.P. Manfredi, D. and Fino, P. (2017), "Investigation of accuracy and dimensional limits of part produced in aluminum alloy by selective laser melting", *The International Journal*

of Advanced Manufacturing Technology, Vol. 88, pp. 451-458. https://doi.org/10.1007/s00170-016-8788-9.

Campanelli, S.L., Contuzzi, N., Angelastro, A. and Ludovico, A.D. (2010), "Capabilities and Performances of the Selective Laser Melting Process", *New Trends in Technologies: Devices, Computer, Communication and Industrial Systems*, Chapter 13, pp. 233-252. https://doi.org/10.5772/10432.

Carmignato, S., De Chiffre, L. , Bosse, H., Leach, R.K., Balsamo, A. and Estler, W.T. (2020), "Dimensional artefacts to achieve metrological traceability in advanced manufacturing", *CIRP Annals*, Vol. 69 No. 2, pp. 693-716. https://doi.org/10.1016/j.cirp.2020.05.009.

Castillo, L. (2005), "Study about the rapid manufacturing of complex parts of stainless steel and titanium", *TNO Industrial Technology*, pp. 1-31. https://www.rm-platform.com/downloads2/send/5-papers/278-study-about-the-rapid-manufacturing-of-complex-parts-of-stainless-steel-and-titanium.

Chahal, V. and Taylor, R.M. (2020), "A review of geometric sensitivities in laser metal 3D printing", *Virtual and Physical Prototyping*, Vol. 15 No. 2, pp. 227-241. https://doi.org/10.1080/17452759.2019.1709255.

Cooke, A.L. and Soons, J.A. (2010), "Variability in the Geometric Accuracy of Additively Manufactured Test Parts", *Proceedings of the 21st Annual International Solid Freeform Fabrication Symposium*, pp. 1-12. https://sffsymposium.engr.utexas.edu/Manuscripts/2010/2010-01-Cooke.pdf.

Das, P., Chandran, R., Samant, R. and Anand, S. (2015), "Optimum Part Build Orientation in Additive Manufacturing for Minimizing Part Errors and Support

Structures", *Procedia Manufacturing*, Vol. 1, pp. 343-354. https://doi.org/10.1016/j.promfg.2015.09.041.

DebRoy, T., Wei, H.L., Zuback, J.S., Mukherjee, T., Elmer, J.W., Milewski, J.O., Beese, A.M., Wilson-Heid, A. and W. Zhang, A. De (2018) "Additive manufacturing of metallic components – Process, structure and properties", *Progress in Materials Science*, Vol. 92, pp. 112-224. https://doi.org/10.1016/j.pmatsci.2017.10.001.

Delgado, J., Ciurana, J., Reguant, C. and Cavallini, B. (2009), "Studying the repeatability in DMLS technology using a complete geometry test part", *Proceedings of the 4th International Conference on Advanced Research in Virtual and Rapid Prototyping VRAP 4*, pp. 349-354.

Ghany, K.A. and Moustafa, S.F. (2006), "Comparison between the products of four RPM systems for metals", *Rapid Prototyping Journal*, Vol. 12 No. 2, pp. 86-94. https://doi.org/10.1108/13552540610652429.

Giganto, S., Martínez-Pellitero, S., Cuesta, E., Meana, V.M. and Barreiro, J. (2020), "Analysis of Modern Optical Inspection Systems for Parts Manufactured by Selective Laser Melting", *Sensors*, Vol. 20 No. 11, pp. 3202. https://doi.org/10.3390/s20113202.

Grimm, T., Wiora, G. and Witt, G. (2015), "Characterization of typical surface effects in additive manufacturing with confocal microscopy", *Surface Topography: Metrology and Properties*, Vol. 3 No. 1, pp. 014001. https://iopscience.iop.org/article/10.1088/2051-672X/3/1/014001.

Hanumaiah, N. and Ravi, B. (2007), "Rapid tooling form accuracy estimation using region elimination adaptive search based sampling technique", *Rapid Prototyping Journal*, Vol. 13 No. 3, pp. 182-190. https://doi.org/10.1108/13552540710750933.

Jiang, X., Ye, T. and Zhu, Y. (2020), "Effect of process parameters on residual stress in selective laser melting of AlSi10Mg", *Materials Science and Technology*, Vol. 36 No. 3, pp. 342-352. https://doi.org/10.1080/02670836.2019.1705560.

Kruth, J.P., Vandenbroucke, B., Van Vaerenbergh, J. and Mercelis, P. (2005), "Benchmarking of different SLS/SLM processes as rapid manufacturing techniques", *Proceedings of the 1st International Conference on Polymers and Moulds Innovations (PMI)*. https://pdfs.semanticscholar.org/6b00/da86b6b2255626058bf1eba918b9ea22c516.pdf?_ga=2.139607611.98309428.1592492320-670251994.1559047744.

Kudzal, A., McWilliams, B., Hofmeister, C., Kellogg, F., Yu, J., Taggart-Scarff, J. and Liang, J. (2017), "Effect of scan pattern on the microstructure and mechanical properties of Powder Bed Fusion additive manufactured 17-4 stainless steel", *Materials & Design*, Vol. 133, pp. 205-215. https://doi.org/10.1016/j.matdes.2017.07.047.

Leach, R.K., Bourell, D., Carmignato, S., Donmez, A., Senin, N. and Dewulf, W. (2019), "Geometrical metrology for metal additive manufacturing", *CIRP Annals*, Vol. 68 No. 2, pp. 677-700. https://doi.org/10.1016/j.cirp.2019.05.004.

Li, C., Liu, J.F., Fang, X.Y. and Guo, Y.B. (2017), "Efficient predictive model of part distortion and residual stress in selective laser melting", *Additive Manufacturing*, Vol. 17, pp. 157-168. https://doi.org/10.1016/j.addma.2017.08.014.

Li, C., Liu, Z.Y., Fang, X.Y. and Guo, Y.B. (2018), "Residual Stress in Metal Additive Manufacturing", *Procedia CIRP*, Vol. 71, pp. 348-353. https://doi.org/10.1016/j.procir.2018.05.039.

Maamoun, A.H., Elbestawi, M., Dosbaeva, G.K. and Veldhuis, S.C. (2018), "Thermal post-processing of AlSi10Mg parts produced by Selective Laser Melting using recycled powder", *Additive Manufacturing*, Vol. 21, pp. 234-247. https://doi.org/10.1016/j.addma.2018.03.014.

Mahesh, M. (2004), "Rapid Prototyping and Manufacturing Benchmarking", Ph.D. thesis, National University of Singapore, Singapore.

Malý, M., Höller, C., Skalon, M., Meier, B., Koutný, D., Pichler, R., Sommitsch, C. and Paloušek, D. (2019), "Effect of Process Parameters and High-Temperature Preheating on Residual Stress and Relative Density of Ti6Al4V Processed by Selective Laser Melting", *Materials*, Vol. 12 No. 6, pp. 930. https://doi.org/10.3390/ma12060930.

Mercelis, P. and Kruth, J.P. (2006), "Residual stresses in selective laser sintering and selective laser melting", *Rapid Prototyping Journal*, Vol. 12 No. 5, pp. 254-265. https://doi.org/10.1108/13552540610707013.

Minetola, P., Galati, M., Calignano, F., Iuliano, L., Rizza, G. and Fontana L. (2020), "Comparison of dimensional tolerance grades for metal AM processes", *Procedia CIRP*, Vol. 88, pp. 399-404. https://doi.org/10.1016/j.procir.2020.05.069.

Moshiri, M., Candeo, S., Carmignato, S., Mohanty, S. and Tosello, G. (2019), "Benchmarking of Laser Powder Bed Fusion Machines", *Journal Manufacturing Materials Processing, Vol.* 3 No. 4, pp. 85. https://doi.org/10.3390/jmmp3040085.

Moylan, S., Slotwinski, J., Cooke, A., Jurrens, K. and Donmez, M.A. (2012), "Proposal for a standardized test artifact for additive manufacturing machines and processes", *Proceedings of the 23th Annual International Solid Freeform Fabrication Symposium*, pp. 902-920. https://tsapps.nist.gov/publication/get_pdf.cfm?pub_id=911953.

Moylan, S., Slotwinski, J., Cooke, A., Jurrens, K. and Donmez, M.A. (2014), "An Additive Manufacturing Test Artifact", *Journal of Research of the National Institute of Standards and Technology*, *Vol.* 119, pp. 429-459. http://dx.doi.org/10.6028/jres.119.017.

Ning, Y., Wong, Y.S., Fuh, J.Y.H. and Loh, H.T. (2006), "An Approach to Minimize Build Errors in Direct Metal Laser Sintering", *IEEE Transactions on Microwave Theory and Techniques*, Vol. 3 No. 1, pp. 73-80. https://doi.org/10.1109/TASE.2005.857656.

Pessard, E., Mognol, P., Hascoët, J.Y. and Gerometta, C. (2008), "Complex cast parts with rapid tooling: rapid manufacturing point of view", *The International Journal of Advanced Manufacturing Technology*, Vol. 39, pp. 898-904. https://doi.org/10.1007/s00170-007-1281-8.

Pidge, P.A. and Kumar, H. (2020), "Additive manufacturing: A review on 3D printing of metals and study of residual stress, buckling load capacity of strut members", *Materials Today: Proceedings*, Vol. 21 No. 3, pp. 1689-1694. https://doi.org/10.1016/j.matpr.2019.12.012.

Rashid, R., Masood, S.H., Ruan, D., Palanisamy, S., Rahman Rashid, R.A., Elambasseril, J. and Brandt, M. (2018), "Effect of energy per layer on the anisotropy of selective

laser melted AlSi12 aluminium alloy", *Additive Manufacturing*, Vol. 22, pp. 426-439. https://doi.org/10.1016/j.addma.2018.05.040.

Rebaioli, L. and Fassi, I. (2017), "A review on benchmark artifacts for evaluating the geometrical performance of additive manufacturing processes", *The International Journal of Advanced Manufacturing Technology*, Vol. 93, pp. 2571-2598. https://doi.org/10.1007/s00170-017-0570-0.

Rivas Santos, V.M., Thompson, A., Sims-Waterhouse, D., Maskery, I., Woolliams, P. and Leach, R. (2020), "Design and characterisation of an additive manufacturing benchmarking artefact following a design-for-metrology approach", *Additive Manufacturing*, Vol. 32, pp. 100964. https://doi.org/10.1016/j.addma.2019.100964.

Rupal, B.S., Ahmad, R. and Qureshi, A.J. (2018), "Feature-Based Methodology for Design of Geometric Benchmark Test Artifacts for Additive Manufacturing Processes", *Procedia CIRP*, Vol. 70, pp. 84-89. https://doi.org/10.1016/j.procir.2018.02.012.

Rupal, B.S., Anwer, N., Secanell, M. and Qureshi, A.J. (2020), "Geometric tolerance and manufacturing assemblability estimation of metal additive manufacturing (AM) processes", *Materials & Design*, Vol. 194, pp. 108842. https://doi.org/10.1016/j.matdes.2020.108842.

Scaravetti, D., Dubois, P. and Duchamp, R. (2008), "Qualification of rapid prototyping tools: proposition of a procedure and a test part", *The International Journal of Advanced Manufacturing Technology*, Vol. 38, pp. 683-690. https://doi.org/10.1007/s00170-007-1129-2.

Strano, G., Hao, L., Everson, R.M. and Evans, K.E. (2013), "Surface roughness analysis, modelling and prediction in selective laser melting", *Journal of Materials Processing Technology*, Vol. 213 No. 4, pp. 589-597. https://doi.org/10.1016/j.jmatprotec.2012.11.011.

Subbaian Kaliamoorthy, P., Subbiah, R., Bensingh, J., Kader, A. and Nayak, S. (2020), "Benchmarking the complex geometric profiles, dimensional accuracy and surface analysis of printed parts", *Rapid Prototyping Journal*, Vol. 26 No. 2, pp. 319-329. https://doi.org/10.1108/RPJ-01-2019-0024.

Sun, Y., Hebert, R.J. and Aindow, M. (2018), "Effect of heat treatments on microstructural evolution of additively manufactured and wrought 17-4PH stainless steel", *Materials & Design*, Vol. 156, pp. 429-440. https://doi.org/10.1016/j.matdes.2018.07.015.

Taylor, H.C., Garibay, E.A. and Wicker, R.B. (2021), "Toward a common laser powder bed fusion qualification test artefact", *Additive Manufacturing*, Vol. 39, pp. 101803. https://doi.org/10.1016/j.addma.2020.101803**.**

Teeter, M.G., Kopacz, A.J., Nikolov, H.N. and Holdsworth, D.W. (2015), "Metrology Test Object for Dimensional Verification in Additive Manufacturing of Metals for Biomedical Applications", *Proceedings of the Institution of Mechanical Engineers, Part H: Journal of Engineering in Medicine, Vol.* 229 No. 1, pp. 20-27. https://doi.org/10.1177/0954411914565222.

Townsend, A., Racasan, R. and Blunt, L. (2018), "Surface-specific additive manufacturing test artefacts", *Surface Topography: Metrology and Properties*, Vol. 6 No. 2, pp. 024007. https://doi.org/10.1088/2051-672X/aabcaf.

Vandenbroucke, B. and Kruth, J.P. (2007), "Selective laser melting of biocompatible metals for rapid manufacturing of medical parts" *Rapid Prototyping Journal*, Vol. 13 No. 4, pp. 196-203. https://doi.org/10.1108/13552540710776142.

Xiao, Z., Chen, C., Hu, Z., Zhu, H. and Zeng, X. (2020), "Effect of rescanning cycles on the characteristics of selective laser melting of Ti6Al4V", *Optics & Laser Technology*, Vol. 122, pp. 105890. https://doi.org/10.1016/j.optlastec.2019.105890.

Yadroitsev, I. and Yadroitsava, I. (2015), "Evaluation of residual stress in stainless steel 316L and Ti6Al4V samples produced by selective laser melting", *Virtual and Physical Prototyping*, Vol. 10 No. 2, pp. 67-76. https://doi.org/10.1080/17452759.2015.1026045.

Yasa, E., Demir, F., Akbulut, F., Cızıoğlu, N. and Pilatin, S. (2014), "Benchmarking of different powder-bed metal fusion processes for machine selection in additive manufacturing", *Proceedings of the 25th Annual International Solid Freeform Fabrication Symposium*, pp. 390-403. http://utw10945.utweb.utexas.edu/sites/default/files/2014-034-Yasa.pdf.

Zapico, P., Giganto, S., Martínez-Pellitero, S., Fernández-Abia, A.I. and Castro-Sastre, M.A. (2018), "Influence of Laser Energy in the Surface Quality of Parts Manufactured by Selective Laser Melting", *Proceedings of the 29th DAAAM International Symposium Intelligent Manufacturing and Automation*, pp. 279-286. https://doi.org/10.2507/29th.daaam.proceedings.040.